Pergamon

Neuroscience Vol. 91, No. 1, pp. 69–80, 1999

PII: S0306-4522(98)00575-2
0306-4522/99 $20.00+0.00

EFFECTS OF NITRIC OXIDE INHIBITION ON THE SPREAD OF BIOTINYLATED DEXTRAN AND ON EXTRACELLULAR SPACE PARAMETERS IN THE NEOSTRIATUM OF THE MALE RAT

A. JANSSON,*† T. MAZEL,‡ B. ANDBJER,* L. ROSÉN,* D. GUIDOLIN,§ M. ZOLI,‖ E. SYKOVÁ,‡ L. F. AGNATI‖ and K. FUXE*

*Department of Neuroscience, Karolinska Institute, S-171 77 Stockholm, Sweden

‡Department of Neuroscience, 2nd Medical Faculty, Charles University and Institute of Experimental Medicine, ASCR, Prague, Czech Republic

§FIDIA Research Laboratories, Abano Terme, Italy

‖Section of Physiology, Department of Biomedical Sciences, University of Modena, Modena, Italy

Abstract—Volume transmission in the brain is mediated by the diffusion of neurotransmitters, modulators and other neuroactive substances in the extracellular space. The effects of nitric oxide synthase inhibition on extracellular space diffusion properties were studied using two different approaches, the histological dextran method and the real-time iontophoretic tetramethylammonium method. The spread of biotinylated dextran (mol. wt 3000) in the extracellular space was measured morphometrically following microinjection into the neostriatum of male rats. Two parameters were used to describe the spread of biotinylated dextran in brain tissue, namely, total volume of spread and the mean grey value. The non-specific nitric oxide synthase inhibitors N^G-nitro-L-arginine methyl ester (10–100 mg/kg) and N^G-monomethyl-L-arginine acetate (30–200 mg/kg) decreased the total volume of spread of dextran in a dose-dependent manner. 7-Nitroindazole monosodium salt (50–100 mg/kg), a specific neuronal nitric oxide synthase inhibitor, did not change the total volume of spread of dextran. Using the tetramethylammonium method, the extracellular space diffusion properties can be described by the volume fraction (α = extracellular space volume/total tissue volume), tortuosity λ (λ^2 = free diffusion coefficient/apparent diffusion coefficient in tissue), and non-specific uptake k' [Nicholson C. and Syková E. (1998) *Trends Neurosci*. **21,** 207–215]. Nitric oxide synthase inhibition by N^G-nitro-L-arginine methyl ester (50 mg/kg) had relatively little effect on volume fraction and tortuosity, and no changes were observed after N^G-monomethyl-L-arginine acetate (20 mg/kg) or 7-nitroindazole monosodium salt (100 mg/kg) treatment. A substantial increase was found only in non-specific uptake, by 13% after N^G-nitro-L-arginine methyl ester and by 16% after N^G-monomethyl-L-arginine acetate, which correlates with the decreased total volume of spread of dextran observed with the dextran method. N^G-Nitro-L-arginine methyl ester treatment (100 mg/kg) decreased striatal blood flow and increased mean arterial blood pressure. The changes in dextran spread and non-specific uptake can be explained by an increased capillary clearance following the inhibition of endothelial nitric oxide synthase, as neuronal nitric oxide synthase inhibition had no effect.

The observed changes after non-specific nitric oxide synthase inhibition may affect the extracellular space concentration of neurotransmitters and modulators, and influence volume transmission pathways in the central nervous system by increased capillary and/or cellular clearance rather than by changes in extracellular space diffusion. © 1999 IBRO. Published by Elsevier Science Ltd.

Key words: neostriatum, extracellular space, vascular permeability, diffusion, volume transmission, nitric oxide synthase.

Intercellular communication in the brain can be classified as wiring transmission and volume transmission (VT).[3,4,15] Wiring transmission includes "private" one-to-one transmission (such as synapses and gap junctions), with little distance between the source and target, and is therefore substantially independent of brain extracellular space (ECS). VT, which is a one-to-many transmission and includes paracrine and endocrine-like transmission in the brain extracellular fluids, is highly dependent on the features of brain ECS.[5] The study of ECS and its changes in different physiological and pathological conditions are therefore of great interest for VT.

Several factors can modify brain ECS and molecular diffusion in it. The ECS volume fraction (α; = ECS volume/total tissue volume, 0.20) and the ECS tortuosity (λ), the ratio of free diffusion coefficient

†To whom correspondence should be addressed.

Abbreviations: α, volume fraction; λ, tortuosity; ADC, apparent diffusion coefficient; CBF, cerebral blood flow; *D*, diffusion coefficient; DAB, 3,3′-diaminobenzidine tetrahydrochloride; ECS, extracellular space; eNOS, endothelial nitric oxide synthase; k', non-specific uptake; L-NAME, N^G-nitro-L-arginine methyl ester; L-NMMA, N^G-monomethyl-L-arginine acetate; MAP, mean arterial blood pressure; MGV_d, mean grey value; 7-NINA, 7-nitroindazole monosodium salt; nNOS, neuronal nitric oxide synthase; NO, nitric oxide; NOS, nitric oxide synthase; TMA^+, tetramethylammonium; V_d, total volume of dextran spread; VT, volume transmission.

(D) to brain apparent diffusion coefficient (ADC): $\lambda = (D/\mathrm{ADC})^{0.5}$, are such factors. In the normal brain, λ varies from 1.5 for small molecules such as transmitters, to 2.5 for large molecules such as albumin.[35] Changes in the morphology and volume of cells, as well as in the composition and concentration of molecules of the extracellular matrix, can modify both α and λ of brain ECS.[35,48] For example, it has been shown that glutamate can cause astroglial swelling and ECS volume decrease.[17] In general, activity decreases ECS volume (see, e.g., the effects of repetitive electrical stimulation in rat spinal cord[46]). On the other hand, clearance of molecules from the ECS depends on uptake by cellular elements, degradation by enzymes and leakage into the blood vessels. Therefore, while diffusion of a given molecule can be controlled by specific mechanisms like uptake or degradation, diffusion of all molecules will be influenced by overall changes in ECS parameters.

Nitric oxide (NO) is a neuromodulator formed by the enzymatic oxidation of L-arginine to L-citrulline. Three isoforms of nitric oxide synthase (NOS) exist. Two of them, endothelial NOS (eNOS) and neuronal NOS (nNOS), are constitutive and calcium/calmodulin-dependent enzymes.[45] The third form, inducible NOS, is found in many cells, including astrocytes and microglia,[33] and is induced by pro-inflammatory events.[45] NO, once synthesized in, e.g., nerve terminals, glial processes or endothelial cells, diffuses in the ECS as well as in the intracellular space towards the target cells, where it increases intracellular guanosine 3′,5′-cyclic monophosphate. NO has been shown to have a broad range of effects in the brain, including effects on cerebral blood flow,[18] capillary permeability,[9,11,21–24,27] vasomotion,[7] blood flow to the plexus choroideus,[13] transmitter release[25] and astroglial function.[6,16,20] All of these effects may influence the size and geometry of the ECS. Therefore, NO, which is by itself a VT signal, is likely to influence diffusion in the ECS of other VT signals through a number of mechanisms.

The NOS inhibitors used in this study rapidly increase systemic blood pressure.[18,39,49] Inhibition of NOS occurs in 40–60 min.[19,26,41] For the full effect of NOS inhibitors to develop, a longer time may be required.[50] Our main interest was, however, in the short-term effects of NOS inhibition, before secondary effects of NOS inhibition develop.

In this study, we examined the effects of NOS inhibitors on the ECS of the striatum, as assessed by morphological measurements of the *in vivo* spread of biotinylated dextran (mol. wt 3000; referred to hereafter as dextran), an ECS marker, and by determining the diffusion parameters of the ECS using the tetramethylammonium (TMA^+) method.[34] Furthermore, some parameters which may alter ECS diffusion (i.e. the state of the blood–brain barrier and cerebral blood flow in the striatum, as well as systemic arterial blood pressure) were also studied following NOS inhibition with N^G-nitro-L-arginine methyl ester (L-NAME) treatment.

EXPERIMENTAL PROCEDURES

Animals

About 150 adult male Sprague–Dawley rats (225–485 g, three to six months old; B&K Universal, Sollentuna, Sweden) were used for this project. The experiments were carried out at the Department of Neuroscience, Karolinska Institute, Stockholm, Sweden (biotinylated dextran spread experiments, cerebral blood flow and morphology) and at the Department of Neuroscience, Prague, Czech Republic (TMA^+ diffusion measurements). In order to use the same strain of rats in the two experimental settings, the required number of rats were sent from Stockholm to Prague. The rats were maintained on a regular light–dark cycle (12 h on/off) in temperature- and humidity-controlled rooms (22–24°C, 30–40% relative humidity), and fed Beekay Rat and Mouse Standard Diet and water *ad libitum*. All possible efforts were made to reduce the number of rats used and to minimize the suffering of the rats. Experimental protocols were approved by the local ethical board in Stockholm (N202/96) and in Prague.

Experimental protocols for biotinylated dextran spread

Stereotactical microinjections. The rats were halothane anaesthetized (2% in the inspired air) and mounted in a stereotactic frame (Kopf Instruments, U.S.A.). A midline incision was made in the skin covering the skull, and a 3-mm hole was made using a dental drill (Messner Emtronic, Dettenhausen, Germany). Microinjections (0.1 μl/2 min) of dextran (1–100 μg/μl) were made stereotactically into the right caudate nucleus (nose = −2.5 mm, bregma = 0.5 mm, lateral = 2.5 mm, ventral = −5.0 mm) using glass micropipettes[54] (tip diameter 50–70 μm) made from 1.5 mm capillaries (Bluebrand/Intramark, Germany). The glass micropipettes were back-filled with dextran (mol. wt 3000, lysine fixable; Molecular Probes, Eugene, OR, U.S.A.; no. D-7135), dissolved in mock cerebrospinal fluid (150 mM Na^+, 3.0 mM K^+, 1.4 mM Ca^{2+}, 0.8 mM Mg^{2+}, 1.0 mM phosphates, 155 mM Cl^-) and connected to a 1-μl Hamilton syringe. The microinjection was controlled by a microinjector pump (CMA100, Carnegie Medicine, Stockholm, Sweden) connected to the Hamilton syringe. A temperature controller (CMA150, Carnegie Medicine) was used to maintain constant body temperature (37 ± 0.5°C). After the microinjection, the wound was closed with three sutures.

Tissue preparation. The experiment was terminated by transcardial perfusion under deep barbiturate anaesthesia (100 mg/kg, i.p., sodium pentobarbital, Apoteksbolaget, Stockholm, Sweden), with 0.9% NaCl solution followed by 8% paraformaldehyde in 0.1 M phosphate buffer (pH 6.9). The brains were dissected out and sliced. Brain slices (bregma ≈ − 1.8 to + 2.7 mm) were postfixed for 60 min and cut as 50-μm-thick sections on a Vibratome (Lancer, St Louis, MO, U.S.A.) and rinsed in 0.1 M phosphate-buffered saline. Every second section was incubated with streptavidin–horseradish peroxidase solution (1:200; Vectastain ABC kit, Vector Laboratories, Burlingame, CA, U.S.A.) for 45 min. These sections were then reacted for 7 min in 50 mM Tris–HCl buffer (pH 7.4) containing the chromogen 3,3′-diaminobenzidine tetrahydrochloride (DAB; 0.2 mg/ml; Sigma no. D-5637) and 0.1 μl/ml H_2O_2 (Perhydrol, Merck, Germany). They were rinsed in 50 mM Tris–HCl buffer (pH 7.4), mounted on gelatin-coated slides, air dried, processed through alcohol/xylene and coverslipped with

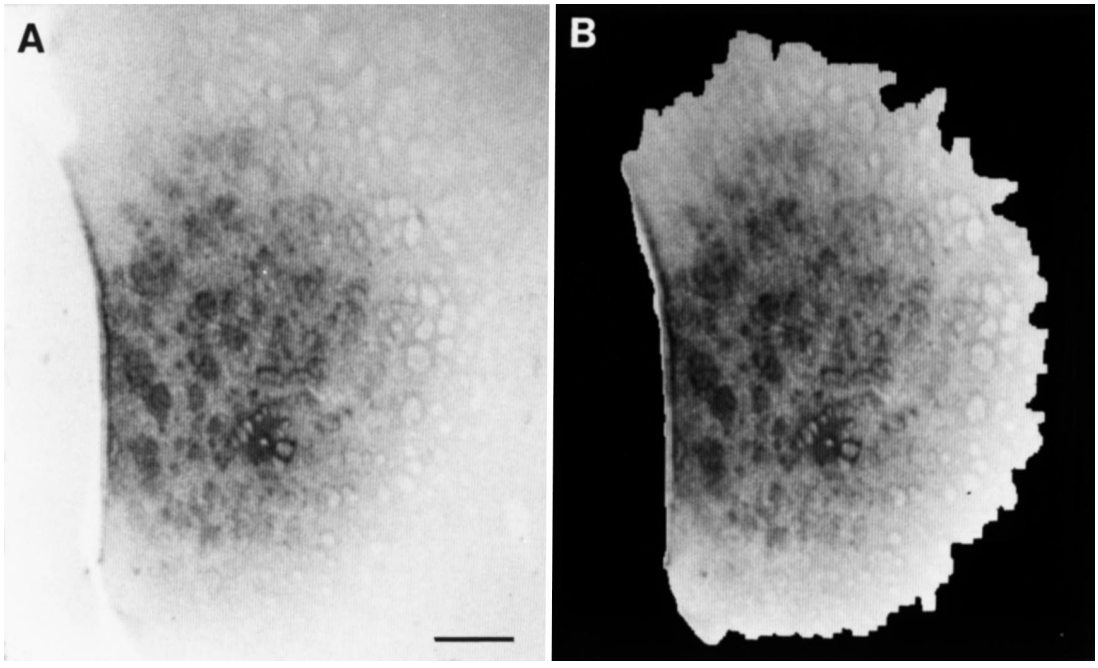

Fig. 1. The spread of biotinylated dextran (mol. wt 3000; 100 nl, 10 μg/μl), 30 min following intrastriatal injection, detected by the streptavidin–horseradish peroxidase/DAB technique. Two pictures from the same representative section are shown with (B) and without (A) the superimposed discrimination frame used for image analysis area determination (Zeiss/Kontron IBAS-system). Scale bar = 500 μm.

Mountex (Histolab, Sweden). Throughout the whole process, the sequence of individual sections was maintained. The possible migration of fixed dextran during the histological preparation is unlikely using 8% paraformaldehyde fixation in combination with lysine-fixable dextran. In any case, the histological preparation was performed using the same time schedule in all brain slices (60 min postfixation, 90 min sectioning, 45 min ABC kit incubation and 7 min in DAB). Every brain was checked for appropriate perfusion by verifying the absence of blood cells in the capillaries of the striatum.

Image analysis. An IBAS image analysis system (Zeiss/Kontron) was used for semi-automatic analysis of the neostriatal sections.[1,55] Images were digitized (512 × 512 pixels/256 grey levels; white = 255/black = 0) into the IBAS system using a Zeiss Axiophot microscope equipped with a Plan-NEOFLUAR 1.25/0.035 objective, yielding a final magnification at the focal plane of × 1.25. Obvious artifacts were interactively erased during the process. An arbitrary but objective criterion (see later) was selected to assess the limits of diffusion of dextran. Thus, an identical automatic procedure was used to determine the discrimination level in all the sections analysed. The background grey level was obtained from a sample of the contralateral striatum of each section. The discrimination level for specific staining was set to a grey value defined as the mean grey value of the background minus 3.0 times the standard deviation of the background grey values[2] (Fig. 1). The specifically stained area was delineated using an erosion/dilation procedure in order to fill small unstained holes and to even the border.[55] The following parameters were calculated for each section series (brain): volume (V_d), estimated from the individual specifically stained areas in the sections measured; mean grey value (MGV_d), the overall median of the mean grey values from the individual specifically stained areas in the sections measured; and form factor, i.e. the ratio between the minimal and maximal axes of the specifically stained area (equal to 1 for a circle and to 0 for a segment).

Time-course and dose–response experiments. To obtain the time-course of spread of dextran, rats were microinjected with dextran (30 μg/μl) and perfused 2, 30, 60 and 120 min (n = 5/group), and 24 h after injection (n = 2). In the dose–response experiment, rats were microinjected with 1, 10, 30 and 100 μg/μl of biotinylated dextran, and perfused 30 min later (n = 5/group).

Nitric oxide synthase inhibition experiments. The protocols used in the NOS inhibitor experiments are presented in Table 1. A concentration of 1 μg/μl of dextran and a time interval of 30 min were chosen for the NOS inhibitor experiments. Rats were injected i.p. with an NOS inhibitor or saline (controls), 10 min prior to the microinjection of dextran into the neostriatum. Thirty min after microinjection, the rats were perfused. The following NOS inhibitors were used: L-NAME (10, 50 and 100 mg/kg), N^G-monomethyl-L-arginine acetate (L-NMMA; 30, 100 and 200 mg/kg) and 7-nitroindazole monosodium salt (7-NINA; 50 and 100 mg/kg) (Tocris Coockson Ltd., Bristol, U.K.). The three NOS inhibitors were given in doses used previously.[12,18,31,32,38,39,41,43,49] L-NAME and L-NMMA have been characterized as non-specific NOS inhibitors, inhibiting all three forms of NOS, although L-NAME shows some specificity towards eNOS.[45] 7-NINA is known to mainly inhibit nNOS.[45] The NOS inhibitors were freshly dissolved and administered in 1 ml saline/rat (0.9% NaCl w/v), except for 7-NINA, which was sonicated in 1 ml of distilled water until completely dissolved.

Tetramethylammonium diffusion measurements

Experiments were performed on 20 rats anaesthetized with an i.p. injection of sodium pentobarbital (65 mg/kg). The skull was opened with a dental drill (bregma = 0.5 mm,

Table 1. Protocol for the nitric oxide synthase inhibition experiments

Experiment	NOS inhibitor	Dose (mg/kg, i.p.)*
Dextran spread†	L-NAME	10, 50, 100
	L-NMMA	30, 100, 200
	7-NINA	50, 100
TMA^+ diffusion parameters‡	L-NAME	50
	L-NMMA	20
	7-NINA	100
Cerebral blood flow§	L-NAME	100
Blood–brain barrier leakage ‖	L-NAME	100

The effects of NOS inhibitors were studied in the following experiments, all performed in the neostriatum of male rats. Dextran spread: the spread of microinjected biotinylated dextran (mol. wt 3000) was semi-quantified by image analysis. TMA^+ diffusion parameters: the diffusion parameters were measured by the real-time iotophoretic TMA^+ method. Cerebral blood flow: the cerebral blood flow was recorded using a laser Doppler flow meter. Blood–brain barrier leakage: morphological evaluation of blood–brain barrier leakage.

*NOS inhibitior was given 10 min before the start of the respective experiment.

†Neostriatal microinjection (0.1 μl) of biotinylated dextran (mol. wt 3000; 1 μg/μl; 30 min duration).

‡Measuring time: 60 min.

§Recording time: 150 min.

‖ Duration of the experiment: 30 min.

lateral = 2.5 mm) and the dura removed. The animal was secured on a heated pad to keep body temperature around 37°C. Artificial cerebrospinal fluid with 1 mM tetramethylammonium chloride heated to 37°C was dripped onto the surface of the exposed skull so as to make a little pool over the brain surface.[52] The animal breathed spontaneously.

ECS diffusion parameters (α, λ and k') were measured using the real-time iontophoretic TMA^+ method. A TMA^+-selective microelectrode was used to measure, in real time, the diffusion profile of an iontophoretically applied ion, TMA^+,[34] that is restricted to the extracellular compartment. Diffusion curves were obtained and the time-dependent rise and fall of the extracellular concentration of TMA^+ was fitted to a radial diffusion equation modified to account for extracellular volume fraction and tortuosity.[34]

Double-barrelled TMA^+-selective electrodes were fabricated as described by Syková.[47] The tip of the TMA^+-sensing barrel was filled with Corning K^+ exchanger 477317 and the rest of the channel was back-filled with 100 mM tetramethylammonium chloride. The reference barrel contained 150 mM NaCl. Iontophoretic micropipettes were prepared from theta glass capillaries. Their shafts were bent so that they could be aligned parallel to those of the TMA^+-selective microelectrodes. They were then back-filled with 100 mM tetramethylammonium chloride. Electrode arrays were made by gluing together an iontophoresis pipette and a TMA^+-selective microelectrode with a tip separation of 100–200 μm. Typical iontophoresis parameters were + 20 nA bias current (continuously applied to maintain a constant transport number), with either + 80- or + 180-nA current steps of 60 s duration to generate the diffusion curve.[52]

Potentials recorded on the reference barrel of the TMA^+-selective microelectrode were subtracted from the ion-selective voltage measurements by means of buffer and subtraction amplifiers. TMA^+ diffusion curves were captured on a digital oscilloscope (Nicolet 310) and then transferred to a PC-compatible, 486 computer, where they were analysed by fitting the data to a solution of the diffusion equation using the program VOLTORO (Nicholson C., unpublished observations).

TMA^+ concentration–time curves were first recorded in 0.3% agar gel (Difco, Agar Noble) in 150 mM NaCl, 3 mM KCl and 1 mM tetramethylammonium chloride to yield electrode transport number and TMA^+ diffusion coefficient. After measuring the reference voltage corresponding to 1 mM TMA^+, the array was lowered to the appropriate depth, and recorded diffusion curves analysed to yield α, λ and non-specific uptake, k' (s^{-1}), in the brain. α, λ and k' in the striatum were determined, and then followed for about 1 h following treatment with an NOS inhibitor. The following treatments were used: L-NAME (50 mg/kg, i.p.), L-NMMA (20 mg/kg, i.p.) or 7-NINA (100 mg/kg, i.p.).

Experimental protocol for striatal blood flow and arterial blood pressure measurements

Rats were halothane anaesthetized during the experiment and respiration maintained via a tracheal cannula connected to an artificial respirator. They were injected with saline (controls) or L-NAME (100 mg/kg, i.p.). Cerebral blood flow (CBF) in the neostriatum and mean arterial blood pressure (MAP) were monitored continuously during 150 min following either treatment. Arterial CO_2 tension (p_aCO_2) and partial pressure of oxygen (p_aO_2) levels were analysed and kept at normo-oxaemia. Body temperature was maintained at 37 ± 0.5°C by means of a heating pad.

The method for CBF has been used previously in our laboratory (for details, see Ref. 51). A laser-Doppler flow meter probe (0.45 mm diameter; PF2B; Perimed, Sweden) was inserted into the neostriatum (coordinates as for dextran microinjections; see above) and the flux signals from the laser-Doppler flowmeter were recorded. The tissue included in the measurement consisted of a hemisphere with a radius of 1 mm.[53] CBF values were expressed as a percentage of the mean value found during the 40 min prior to treatment (baseline). No absolute blood flow values in ml/min can be obtained using this technique.[42]

MAP was monitored continuously by means of a heparinized plastic catheter (PE-50) inserted into the common carotid artery, connected to a Statham PC23 d.c. transducer (Statham, Puerto Rico) and a pen recorder. MAP values were expressed as a percentage of the baseline mean value (40 min) prior to treatment.

Experimental protocol to visualize blood–brain barrier leakage

Forty minutes after treatment with saline (1 ml, i.p.), L-NAME (100 mg/kg, i.p.) or L-phenylephrine (20 μg/kg/min for 5 min, i.v.) (n = 3 in each group) rats were deeply

Table 2. Time-course and dose–response for spread of biotinylated dextran (mol. wt 3000) microinjected into the neostriatum: microdensitometrical and morphometrical parameters using the discriminative method

		Volume V_d (mm^3)	Mean grey value (MGV_d)	Form factor
Time (min)	2	16 ± 2	30 ± 3	0.65 ± 0.03
	30	43 ± 6[a]	30 ± 2	0.78 ± 0.01[c]
	60	56 ± 3[a]	25 ± 1	0.78 ± 0.02[c]
	120	66 ± 15[a]	21 ± 2[b]	0.77 ± 0.01[c]
Dose (μg/μl)	1	20 ± 3	24 ± 3	0.82 ± 0.02
	10	21 ± 4	24 ± 2	0.78 ± 0.02[f]
	30	50 ± 3[d]	32 ± 2[e]	0.81 ± 0.01
	100	54 ± 8[d]	28 ± 1	0.81 ± 0.01

The time-course and dose–response relationship for the spread of biotinylated dextran (mol. wt 3000) microinjected into the neostriatum. The rats were halothane anaesthetized and dextran was microinjected in 0.1 μl of mock cerebrospinal fluid. A concentration of 30 μg/μl of biotinylated dextran and a 30-min time interval were used in the time-course and dose–response experiments, respectively. The following parameters were calculated for each section series (brain): volume (V_d), estimated from the individual specifically stained areas in the sections measured; mean grey value (MGV_d), the overall median of the mean grey values from the individual specifically stained areas in the sections measured; form factor, i.e. overall ratio between the minimal and maximal perpendicular length of the specifically stained area. Data are presented as means ± S.E.M.; $n = 5$ in each group. One-way ANOVA followed by Fisher's PLSD post hoc comparison was used in the statistical analysis. $P < 0.05$ was considered a statistically significant difference. Statistically significant trends ($P < 0.05$) were found for V_d of the time-course and dose response and for the form factor of the time-course, using a Jonckheere–Terpstra trend test. [a,c]Different from 2 min; [b]different from 2 and 30 min; [d]different from 1 and 10 μg/μl groups; [e]different from 1 and 10 μg/μl groups; [f]different from 1 μg/μl group.

anaesthetized (pentobarbital) and killed by transcardial perfusion of saline (50 ml), followed by fixative (100 ml; 4% paraformaldehyde and 0.2% picric acid in 0.1 M phosphate buffer, pH 6.9). Slices of the brains were kept in the fixative for 90 min and then immersed in 10% sucrose in 0.1 M phosphate buffer. Vascular protein leakage was visualized by immunocytochemistry. Two primary antibodies were used, biotinylated anti-rat immunoglobulin G (1:100; Vector) and rabbit anti-rat albumin (1:250; Nordic), followed by an ABC kit (Vector) with DAB as chromogen. Three rats were given 3 ml/kg of 2% Evan's Blue in 0.9% NaCl (i.v.) 20 min before treatment.

Statistical analysis

The statistical analysis of the dose–response, time-course and NOS inhibitor experiments was carried out by means of a one-way ANOVA followed by Fisher's PLSD test, and also further analysed with a Jonckheere–Terpstra trend test. Student's *t*-test was used for the electrophysiological experiments. In order to compare the integrated (area under the curve) values and peak values of the CBF/MAP curves, the Mann–Whitney *U*-test was used. Data are presented as means ± S.E.M. $P < 0.05$ was considered to be a statistically significant difference.

RESULTS

Spread of biotinylated dextran

The volume (V_d) of labelled dextran (30 μg/μl) in the neostriatum increased from 2 to 120 min post-injection (from 16 ± 2 to 66 ± 15 mm^3), and the MGV_d values decreased from 30 ± 3 to 21 ± 2 (Table 2, Fig. 1). Significant differences were found for the V_d, MGV_d and form factor parameters, when analysing the time-course data with a one-way ANOVA. A significant monotonic trend ($P < 0.05$, Jonckheere–Terpstra test) toward an increase was found for the V_d and form factor, but not for MGV_d (Table 2). At the 24-h time interval, the V_d was very low, namely 1.8 ± 0.3 mm^3, the MGV_d was 23 ± 2 and the form factor was 0.47 ± 0.1 ($n = 2$).

In the dose–response experiment, using doses of dextran from 1 up to 100 μg/μl, the volume (V_d) of labelled dextran in the neostriatum increased significantly, from 20 ± 3 to 54 ± 8 mm^3, in a dose-dependent manner, 30 min following microinjection (Table 2). In the same experiment, the MGV_d parameter increased from 24 ± 3 to 32 ± 2 (30 μg/μl). Statistically significant differences were found for the V_d, MGV_d and form factor parameters, when analysing the dose–response data with a one-way ANOVA. A significant monotonic trend ($P < 0.05$, Jonckheere–Terpstra test) toward an increase was found for the V_d, but not for the MGV_d and form factor (Table 2).

Effects of nitric oxide synthase inhibition on the spread of biotinylated dextran

L-NAME treatment with 50 or 100 mg/kg, but not with 10 mg/kg, significantly decreased the V_d of labelled dextran to 65 ± 2% and 63 ± 4%, respectively, of control value in the neostriatum 30 min after microinjection. In the same experiment, MGV_d decreased significantly to 60 ± 11% of control value by L-NAME treatment (50 mg/kg). The form factor was not changed by any dose of L-NAME treatment (Fig. 2A).

L-NMMA treatment with 30, 100 or 200 mg/kg significantly decreased the V_d of labelled dextran to 58 ± 11%, 48 ± 10% and 52 ± 7% of control value, respectively, 30 min after microinjection into

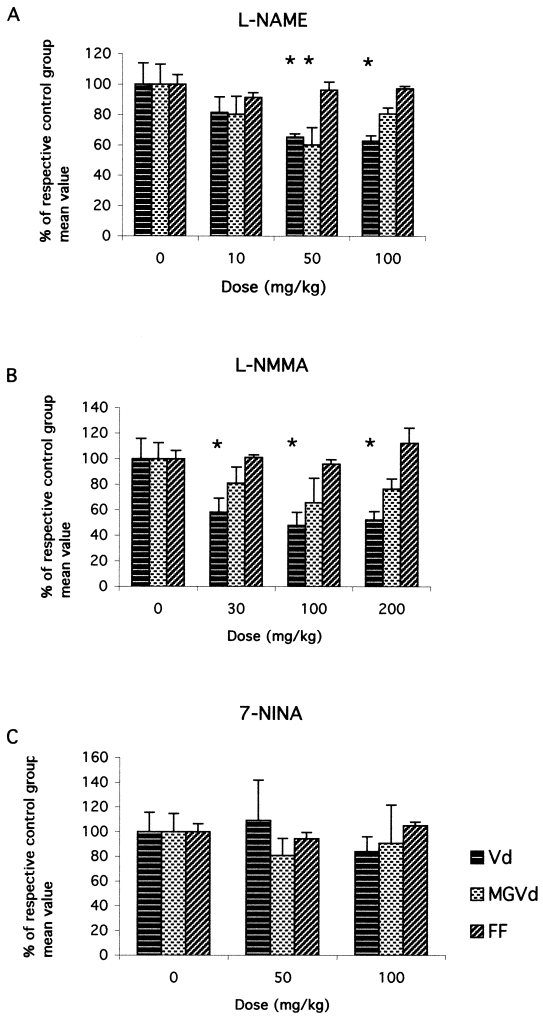

Fig. 2. Dose-related effects of NOS inhibition on the spread of biotinylated dextran (mol. wt 3000), following microinjection into the neostriatum. When analysing the spread of dextran, it was found that the total volume (V_d) decreased dose-dependently and significantly following L-NAME (A) and L-NMMA (B) treatment, but not after 7-NINA (C) treatment. L-NAME treatment decreased MGV_d significantly (A; $P < 0.05$). The form factor (FF) was not changed by L-NAME, L-NMMA or 7-NINA treatment. The rats were given saline (control), L-NAME, L-NMMA or 7-NINA 10 min prior to the dextran microinjection, and 30 min after the microinjection the rats were killed. Dextran was visualized with streptavidin–horseradish peroxidase using DAB as chromogen in serial sections (50 μm/1:2 sections) throughout the neostriatum. V_d, MGV_d and form factor for the specific labelling following microinjection of dextran were determined by image analysis. The graphs show the mean relative change compared to respective control value ± S.E.M. ($n =$ 3–5 in each group). Statistical analysis was made with a one-way ANOVA followed by a PLSD test (*$P < 0.05$). Mean baseline values (V_d; MGV_d; form factor; for variability, see figure): L-NAME treatment (26 mm^3; 26; 0.79), L-NMMA treatment (16 mm^3; 20; 0.79), 7-NINA treatment (18 mm^3; 22; 0.79).

the neostriatum. In the same experiment, the MGV_d was reduced, although not significantly, by L-NMMA treatment (100 and 200 mg/kg). The form factor was not changed by L-NMMA treatment (Fig. 2B).

7-NINA treatment with 50 or 100 mg/kg did not change the V_d, MGV_d or form factor parameters of dextran 30 min after microinjection into the neostriatum (Fig. 2C).

Tetramethylammonium diffusion parameters in the neostriatum following nitric oxide synthase inhibition

TMA^+ diffusion curves were recorded at various depths of the striatum. The electrodes were inserted 2.9 mm below the surface of the brain and diffusion curves were taken every 0.2 mm down to a depth of 3.7 mm. All measurements were made with the tips of the electrodes aligned transverse to the sagittal suture. Diffusion parameters did not vary with depth. Volume fraction (α) in the striatum was 0.22 ± 0.007 (mean ± S.E.M.), tortuosity $\lambda =$ 1.60 ± 0.02 and non-specific uptake $k' = 5.8 \pm 0.6$ (10^{-3} s^{-1}). After several control measurements, the NOS inhibitor was given (i.p.) and the diffusion parameters followed for about 1 h. Diffusion curves were taken at 5-min intervals. Figure 3A, C and D shows the time-course of α, λ and k' following L-NAME treatment. For statistical analysis, the mean of all measurements 0–30 min before the NOS inhibitor application (control value) was compared with the mean of measurements made in the time interval of maximal response after the treatment (Table 3, Fig. 3B). Following L-NAME (50 mg/kg) treatment, volume fraction, tortuosity and non-specific uptake increased significantly, while following L-NMMA (20 mg/kg), only the non-specific uptake increased significantly. However, with L-NAME, the changes in volume fraction (8%) and tortuosity (2%, i.e. a 4% decrease in ADC) were relatively small. 7-NINA (100 mg/kg) treatment did not significantly change any of the diffusion parameters. The possible effect of the observed changes on the TMA^+ and possibly also the dextran spread can be demonstrated using TMA^+ isoconcentration spheres, representing surfaces where TMA^+ reaches a concentration of 0.1 μM 10 min after its iontophoretic application ($I = 180 \times 10^{-9}$ A, 60 s) in the centre of the sphere (Fig. 3E, F). The sphere after L-NAME treatment is smaller, i.e. TMA^+ spread is reduced. A similar change could be demonstrated for L-NMMA, although the most important factor was the increase in uptake.

Effects of nitric oxide synthase inhibition on striatal blood flow and mean arterial blood pressure

Treatment with L-NAME (100 mg/kg) slowly reduced the relative CBF during 150 min (Fig. 4A). When considering the percentage CBF change (%CBF) integrated over time (area under the curve), a significant decrease was found. During 150 min, the relative MAP increased significantly (%MAP change integrated over time) following L-NAME

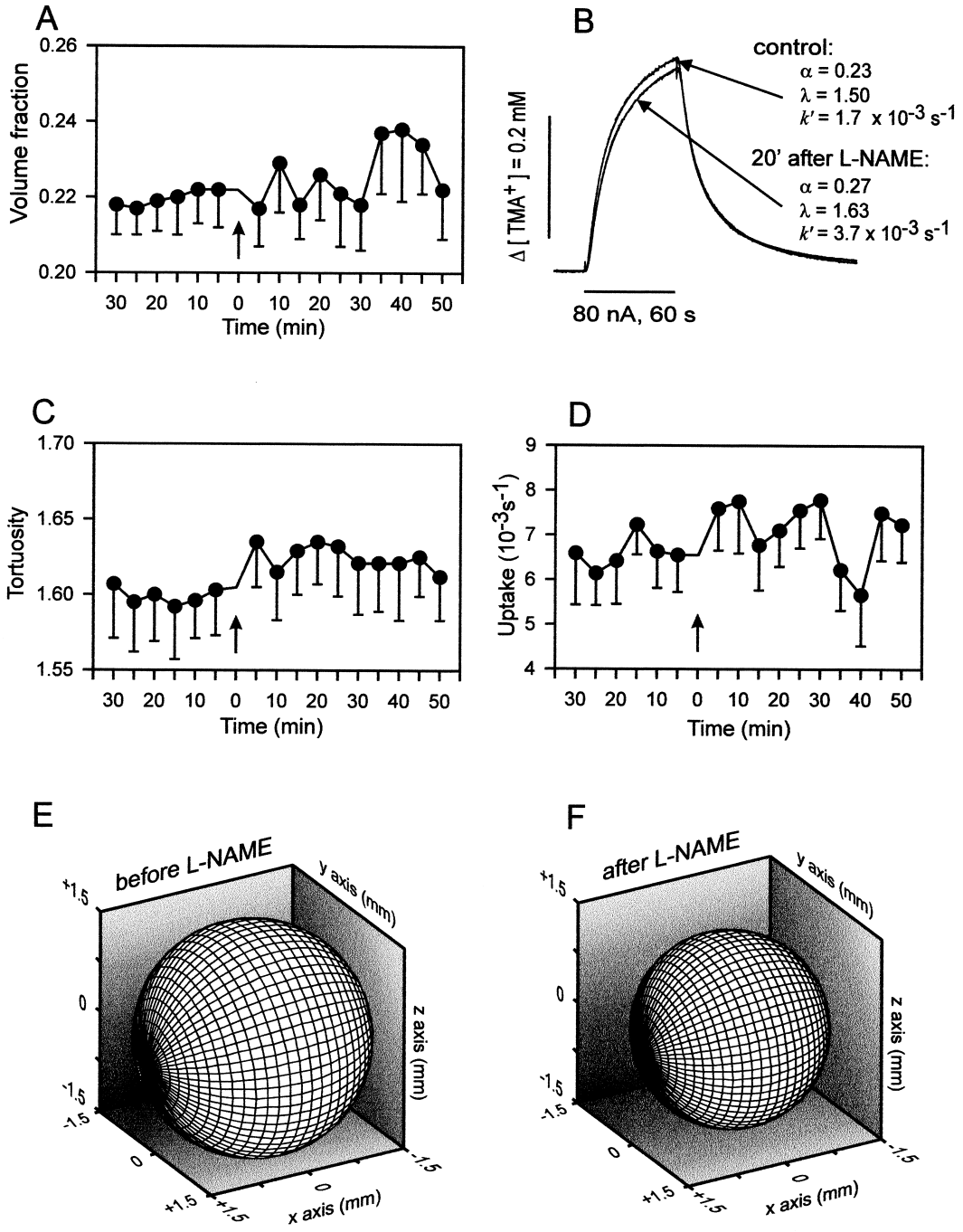

Fig. 3. Neostriatal ECS diffusion parameters measured with the real-time iontophoretic TMA^+ method following L-NAME treatment (50 mg/kg, i.p.). (A, C, D) Time-course of volume fraction (α), tortuosity (λ) and non-specific uptake (k') before and after L-NAME application. Maximal changes in λ and k' were found 10–30 min after L-NAME application. Maximal changes were observed 30–40 min after the treatment. Data presented as mean ± S.E.M. ($n = 14$). (B) Two characteristic TMA^+ diffusion curves (control and L-NAME treatment, 20 min), together with the respective values for α, λ and k'. (E, F) Isoconcentration spheres representing surfaces where TMA^+ reaches an extracellular concentration of 0.1 μM 10 min after its application ($I = 180 \times 10^{-9}$ A, 60 s) in the centre of the sphere. Mean values of the ECS diffusion parameters (α, λ and k') before and after L-NAME treatment (see Table 3), as well as parameters typical for TMA^+ measurements ($D = 1.311 \times 10^{-9}$ m^2/s at 37°C, $n = 0.3$; D = diffusion coefficient, n = transport number), were used. The isoconcentration sphere after L-NAME treatment is smaller than the isoconcentration sphere before the treatment.

Table 3. Effects of nitric oxide synthase inhibition on the striatal diffusion parameters

Treatment	Parameter	Control value	Maximal response
L-NAME (50 mg/kg)	α	0.22 ± 0.01	0.24 ± 0.01*
	λ	1.59 ± 0.02	1.62 ± 0.03*
	k'	6.4 ± 0.7	7.2 ± 0.8*
L-NMMA (20 mg/kg)	α	0.23 ± 0.01	0.23 ± 0.01
	λ	1.61 ± 0.01	1.63 ± 0.01
	k'	6.1 ± 0.4	7.1 ± 0.2*
7-NINA (100 mg/kg)	α	0.20 ± 0.01	0.20 ± 0.01
	λ	1.63 ± 0.01	1.60 ± 0.02
	k'	4.2 ± 0.9	2.9 ± 0.4

Striatal diffusion parameters were measured using the real-time iontophoretic TMA^+ method. The mean of all measurements 0–30 min before NOS inhibitor application (control value) was compared with the mean of measurements made in the time interval of maximal response after the treatment. All values are expressed as mean ± S.E.M. Paired Student's *t*-test was used for statistical analysis in the case of L-NAME ($n = 14$) treatment. For L-NMMA ($n = 11$) and 7-NINA ($n = 8$), unpaired *t*-test was used. Significant changes are marked with asterisks ($P < 0.05$). α, volume fraction; λ, tortuosity; k', non-specific uptake (10^{-3} s^{-1}); *n*, number of measurements.

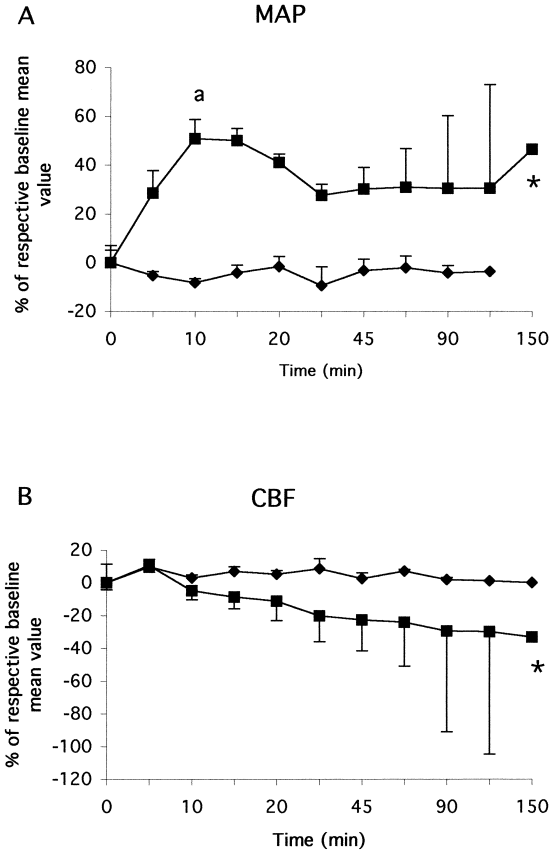

Fig. 4. Effects of systemic L-NAME (100 mg/kg) treatment on striatal blood flow (CBF; A) and MAP (B). Following L-NAME treatment, CBF decreased significantly and MAP increased significantly compared to saline-treated controls. The values are shown as a percentage of the respective baseline value (mean ± S.E.M.). Filled diamonds indicate control and filled squares indicate L-NAME treatment; $n = 3$ or 4 in each group. A comparison of the total area under the curve for each treatment was made with a Mann–Whitney *U*-test (*$P < 0.05$). a, MAP peak value different from control ($P < 0.05$). Baseline values were: for saline treatment (CBF; MAP), 12 ± 3 LDF units; 68 ± 3 mmHg; for L-NAME treatment (CBF; MAP), 16 ± 1 LDF units; 72 ± 3 mmHg.

treatment (Fig. 4B). The increase in MAP was rapid, with a significant maximal change at 10 min (+51%), and outlasted the observation period (150 min).

Evaluation of vascular protein leakage

The effects of L-NAME treatment on the blood–brain barrier were evaluated by visualizing the leakage of blood proteins into the cerebral ECS. As a comparison, the effects of a hypertensive treatment known to increase the vascular permeability (phenylephrine, 20 μg/min, 5 min)[27] and reported to increase MAP by the order of 50%[44] were evaluated. In the dextran experiments, the rats were killed 40 min after NOS inhibitor injection. Therefore, a similar time interval was used in this experiment. Vascular permeability was not substantially increased by L-NAME or phenylephrine, as visualized by rat albumin immunoreactivity or Evan's Blue fluorescence (Fig. 5). Analysis of rat immunoglobulin G immunoreactivity gave similar results (data not shown).

DISCUSSION

The present paper analyses the influence of NOS inhibition on ECS diffusion parameters by measuring the spread of biotinylated dextran (mol. wt 3000) in brain tissue *in vivo* and the diffusion of TMA^+. Dextran has been used in the study of the ECS. Nicholson and Tao,[36] as well as Bjelke *et al.*,[8] have studied how macromolecules like albumins and dextrans with different molecular weights migrate in the ECS.[35] NO has been shown to regulate processes like capillary permeability[9,11,21–24,27] and astroglial function.[6,16,20] Therefore, NO could influence the size and geometry of the ECS and modulate the spread of macromolecules.

The dose–response and time-course experiments

of the present study were performed to estimate the effect of NOS inhibition on the spread of dextran. With time, there is a significant increase in V_d and a decrease in MGV_d, indicating a spread of dextran *in vivo* in the neostriatum. Injections of increasing concentrations of dextran result in a larger V_d and a higher MGV_d (Table 2). Quenching of the signals could explain why there is no further increase in the V_d and MGV_d following injection of 100 μg/μl of biotinylated dextran compared to the dose of 30 μg/μl. To avoid quenching, a low dose of dextran (1 μg/μl) was used in the NOS inhibitor experiments. The form factor values show that there is an anisotropic diffusion of dextran along the needle tract, since the values are lower than 1. This anisotropy is most clearly evident at 2 min, when the form factor is significantly reduced compared to the longer time intervals. These results indicate that the ECS is available for the spread of dextran, as demonstrated previously *in vitro*,[36] and that the *in vivo* spread of dextran may be semi-quantified by this method.

Influence of nitric oxide synthase inhibition on dextran spread

A substantial reduction of the total volume of dextran was demonstrated following acute L-NAME and L-NMMA treatment. 7-NINA treatment did not alter the total volume of labelled dextran. Treatment with L-NAME or L-NMMA inhibits all three isoforms of NOS, while 7-NINA mainly inhibits nNOS.[45] Since only a small contribution of NO comes from inducible NOS in the normal brain, the main difference between these treatments is the inhibition of eNOS by L-NAME/L-NMMA but not by 7-NINA. That both L-NAME and L-NMMA are effective in V_d reduction also makes it unlikely that non-specific effects of the drugs, such as a muscarinic antagonistic effect of L-NAME,[10] contribute to the observed effect.

Overall, our data suggest that eNOS and the subsequent reduction in vascular NO production results in an increased leakage of dextran from the ECS to the lumen of the brain capillaries. This would explain the reduction of total labelled dextran volume found after L-NAME/L-NMMA treatment. Increased clearance to the blood is also consistent with the finding of significant decreases in dextran concentration in brain ECS as evaluated by a decrease in MGV_d. The observed change in MGV_d is dependent on an accurate determination of this parameter. Another interpretation cannot be excluded, e.g., an increase in tortuosity alone, but this is less likely in view of the results obtained with the TMA^+ method (see below).

The interpretation favoured in this paper is apparently in disagreement with previous results on the effects of NOS inhibition on vascular permeability, in which acute hypertension-,[27] glutamate-[30] or histamine-induced[28] increases in vascular permeability were reduced by NOS inhibition. However, these experiments are only partly comparable with the present study. First, we did not use a pathological model (hypertension or inflammation); second, we suggest a change in brain to blood permeability and not the opposite. The present results are more in agreement with the papers by Kubes[21] and Kurose *et al.*,[24] in which increased intestinal capillary permeability followed NOS inhibition. In this comparison, however, the differences between brain and intestinal capillaries must be considered. To further evaluate the effects of NOS inhibition on the blood–brain barrier, dextran could have been systemically administered and detected in the brain tissue,[28] but that was beyond the scope of this investigation.

In line with previous results,[18] L-NAME decreased the striatal blood flow and increased systemic MAP. These changes may, at least partly, contribute to the changes observed in the spread of dextran. However, a decreased CBF alone should result in an increased retention of dextran in the brain tissue due to reduced flow in the capillary bed, and therefore increases in V_d and MGV_d. However, in the dextran experiments, using two different NOS inhibitors, the opposite effect was found, namely a decrease in V_d and MGV_d. Furthermore, we could not find any brain leakage of blood proteins 30 min after NOS inhibition or after a pharmacological treatment (phenylephrine) which causes an increase in MAP comparable to that of L-NAME. This last result may, however, be partly dependent on the relative insensitivity of our methods and on the large size of these proteins compared with dextran (mol. wt 3000), and with another method, increased penetration of fluorescent albumin over the blood–brain barrier following phenylephrine-induced hypertension has been shown.[29] The influence of blood flow and blood pressure changes on the present results is therefore probably not critical.

Influence of nitric oxide synthase inhibition on extracellular space diffusion parameters measured using the tetramethylammonium method

The diffusion parameters in the striatum that we obtained with the real-time iontophoretic TMA^+ method closely resemble those obtained previously with radiotracer methods *in vivo*[14,37] and with the TMA^+ method in brain slices.[40] After L-NAME treatment, ECS volume fraction α, tortuosity λ and non-specific uptake k' were slightly, but significantly ($P < 0.05$), increased. After L-NMMA, only non-specific uptake k' increased significantly, whereas after 7-NINA treatment no changes were observed. As discussed earlier, these changes are probably due to eNOS inhibition.

We may try to estimate the influence of these

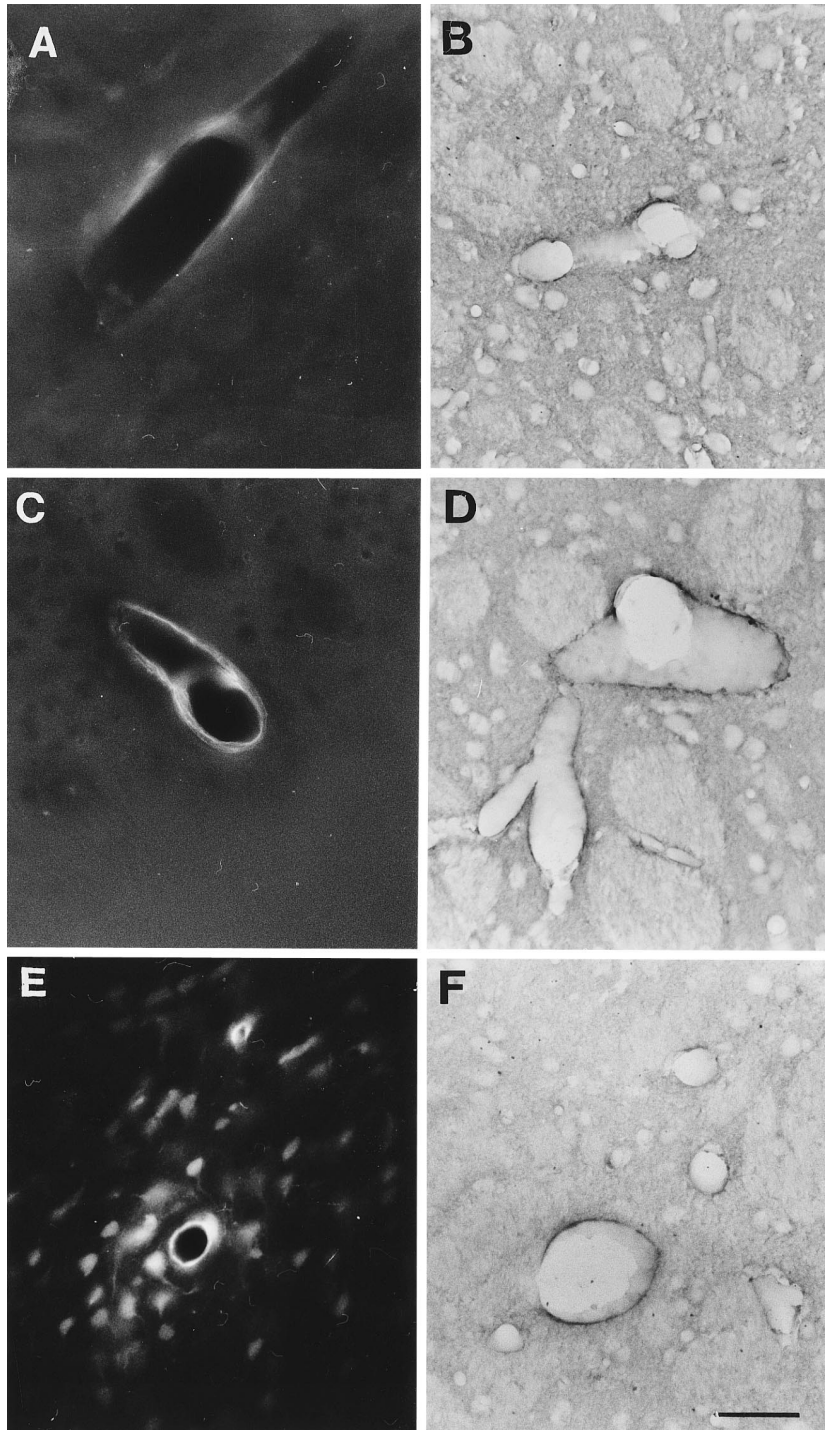

Fig. 5. The effects of saline (A, B), L-NAME (C, D) or phenylephrine (E, F) treatment on perivascular Evan's Blue fluorescence (A, C, E) and rat albumin immunoreactivity (B, D, F), 30 min after respective treatment. Systemic L-NAME treatment (30 min, 100 mg/kg, i.p.) was compared with a treatment known previously to disrupt the blood–brain barrier due to acute hypertension (phenylephrine, 20 μg/kg/min, 5 min, i.v.). Saline-treated rats served as controls. There is an increased labelling of endothelial cells with both treatments compared to saline, and a minor vascular leakage was shown following phenylephrine treatment (E).

changes on dextran spread after NOS inhibitor treatment (Fig. 3E, F). The increase in volume fraction (8% after L-NAME) is small and has no direct effect on dextran spread. The increase in tortuosity (2% for L-NAME, i.e. a 4% change in the TMA^+ apparent diffusion coefficient) is too small to have any detectable influence. The only larger change after both L-NMMA and L-NAME treatment is the increase in

non-specific uptake (13% for L-NAME and 16% for L-NMMA). The observed increase in non-specific TMA^+ uptake may represent either increased uptake by cells or increased clearance over the blood vessels. Increased uptake leads to a reduction of TMA^+ diffusion and could lead to a reduction in dextran spread (in the time scale used, i.e. a 30-min dextran spread; see Fig. 3E, F). If, in this experimental model, increased non-specific uptake is due to increased clearance to the blood, this effect could also explain the observed decrease in MGV_d. Thus, we may conclude that the observed changes in dextran spread best correlate with the increase in uptake.

CONCLUSION

Inhibition of NOS by L-NAME and L-NMMA, i.e. decreased endogenous NO production, leads to a decrease in dextran spread and a decrease in MGV. This may be explained by an increase in dextran capillary clearance. Endothelial NOS may be important in mediating this effect since 7-NINA, an nNOS inhibitor, was without effect. In support of this hypothesis, both L-NAME and L-NMMA produce a substantial increase in non-specific TMA^+ uptake. L-NAME treatment increased ECS volume fraction and tortuosity to a relatively small extent, and L-NMMA was ineffective in this respect. Taken together, by regulating vascular permeability from the brain parenchyma to the vessels, endothelial NO may possibly be involved in the regulation of volume transmission in the brain.

Acknowledgements—This work was supported by a grant (04X-715) from the Swedish Medical Research Council. We also gratefully acknowledge the support from the Marcus and Marianne Wallenberg Foundation, GACR 309/96/0886 and IGAMZ 3423-3, and from Stiftelsen Lars Hiertas minne. We are grateful to Ms Annica Andersson for expert technical assistance and to Dr Richard Orkand for his comments on the manuscript.

REFERENCES

1. Agnati L. F. and Fuxe K. (1985) *Quantitative Neuroanatomy in Transmitter Research, Wenner-Gren International Symposium Series*. Macmillan, London.
2. Agnati L. F., Fuxe K., Benfenati F., Zini I., Zoli M., Fabbri L. and Härfstrand A. (1984) Computer assisted morphometry and microdensitometry of transmitter identified neurons with special reference to the mesostriatal dopamine pathway. I. Methodological aspects. *Acta physiol. scand.* **532** (Suppl.), 5–32.
3. Agnati L. F., Fuxe K., Merlo-Pich E., Zoli M., Zini I., Benfenati F., Härfstrand A. and Goldstein M. (1987) Aspects on the integrative capabilitites of the central nervous system: evidence for "volume transmission" and its possible relevance for receptor–receptor interactions. In *Receptor–Receptor Interactions* (eds Fuxe K. and Agnati L. F.), pp. 236–249. Macmillan, London.
4. Agnati L. F., Fuxe K., Zoli M., Zini I., Toffano G. and Ferraguti F. (1986) A correlation analysis of the regional distribution of central enkephalin and β-endorphin immunoreactive terminals and of opiate receptors in adult and in old male rats. Evidence for the existence of two types of communication in the central nervous system: the volume transmission and the wiring transmission. *Acta physiol. scand.* **128**, 201–207.
5. Agnati L. F., Zoli M., Strömberg I. and Fuxe K. (1995) Intercellular communication in the brain: wiring versus volume transmission. *Neuroscience* **69**, 711–726.
6. Asano S., Matsuda T., Takuma K., Kim H. S., Sato T., Nishikawa T. and Baba A. (1995) Nitroprusside and cyclic GMP stimulate Na^+–Ca^{2+} exchange activity in neuronal preparations and cultured rat astrocytes. *J. Neurochem.* **64**, 2437–2441.
7. Bertuglia S., Colantuoni A. and Intaglietta M. (1994) Effects of L-NMMA and indomethacin on arteriolar vasomotion in skeletal muscle microcirculation of conscious and anesthetized hamsters. *Microvasc. Res.* **48**, 68–84.
8. Bjelke B., England R., Nicholson C., Rice M. E., Lindberg J., Zoli M., Agnati L. F. and Fuxe K. (1995) Long distance pathways of diffusion for dextran along fibre bundles in brain. Relevance for volume transmission. *NeuroReport* **6**, 1005–1009.
9. Boje K. M. K. (1995) Inhibition of nitric oxide synthase partially attenuates alterations in the blood–cerebrospinal fluid barrier during experimental meningitis in the rat. *Eur. J. Pharmac.* **272**, 297–300.
10. Buxton I. L., Cheek D. J., Eckman D., Westfall D. P., Sanders K. M. and Keef K. D. (1993) N^G-Nitro-L-arginine methyl ester and other alkyl esters are muscarinic receptor antagonists. *Circulation Res.* **72**, 387–395.
11. Chi O. Z., Chang Q., Wang G. and Weiss H. R. (1997) Effects of nitric oxide on blood–brain barrier disruption caused by intracarotid injection of hyperosmolar mannitol in rats. *Anesth. Analg.* **84**, 370–375.
12. Connop B. P., Rolfe N. G., Boengman R. J., Jhamandas K. and Beninger R. J. (1994) Potentiation of NMDA-mediated toxicity on nigrostriatal neurons by a low dose of 7-nitroindazole. *Neuropharmacology* **33**, 1439–1445.
13. Faraci F. M. (1992) Regulation of the cerebral circulation by endothelium. *Pharmac. Ther.* **56**, 1–22.
14. Fenstermacher J. D. and Kaye T. (1988) Drug "diffusion" within the brain. *Ann. N. Y. Acad. Sci.* **531**, 29–39.
15. Fuxe K., von Euler G. and Agnati L. F. (1988) Studies on central D1 receptors' role in volume transmission, neuroendrocrine regulation and release of noradrenaline. *Adv. exp. Med. Biol.* **235**, 83–119.
16. Garg U. C., Devi L., Turndorf H., Goldfrank L. R. and Bansinath M. (1992) Effect of nitric oxide on mitogenesis and proliferation of cerebellar glial cells. *Brain Res.* **592**, 208–212.
17. Hansson E. and Ronnback L. (1995) Astrocytes in glutamate neurotransmission. *Fedn Proc. Fedn Am. Socs exp. Biol.* **9**, 343–350.
18. Iadecola C., Pellegrino D. A., Moskowitz M. A. and Lassen N. A. (1994) Nitric oxide synthase inhibition and cerebrovascular regulation. *J. cerebr. Blood Flow Metab.* **14**, 175–192.
19. Iadecola C., Xu X., Zhang F., Hu J. and el-Fakahany E. E. (1994) Prolonged inhibition of brain nitric oxide synthase by short-term systemic administration of nitro-L-arginine methyl ester. *Neurochem. Res.* **19**, 501–505.
20. Ishizaki Y., Ma L. J., Morita I. and Murota S. (1991) Astrocytes are responsive to endothelium-derived relaxing factor (EDRF). *Neurosci. Lett.* **125**, 29–30.

21. Kubes P. (1992) Nitric oxide modulates epithelial permeability in the feline small intestine. *Am. J. Physiol.* **262**, G1138–G1142.
22. Kubes P. (1993) Nitric oxide-induced microvascular permeability alterations: a regulatory role for cGMP. *Am. J. Physiol.* **265**, H1909–H1915.
23. Kubes P. and Granger D. N. (1992) Nitric oxide modulates microvascular permeability. *Am. J. Physiol.* **262**, H611–H615.
24. Kurose I., Wolf R., Grisham M. B., Aw T. Y., Specian R. D. and Granger D. N. (1995) Microvascular responses to inhibition of nitric oxide production. Role of active oxidants. *Circulation Res.* **76**, 30–39.
25. Liu Y. (1996) Nitric oxide influences dopaminergic processes. *Adv. Neuroimmun.* **6**, 259–264.
26. MacKenzie G. M., Rose S., Bland-Ward P.A., Moore P. K., Jenner P. and Marsden C. D. (1994) Time course of inhibition of brain nitric oxide synthase by 7-nitro indazole. *NeuroReport* **5**, 1993–1996.
27. Mayhan W. G. (1995) Nitric oxide in the disruption of the blood–brain barrier during acute hypertension. *Brain Res.* **686**, 99–103.
28. Mayhan W. G. (1996) Role of nitric oxide in histamine-induced increases in permeability of the blood–brain barrier. *Brain Res.* **743**, 70–76.
29. Mayhan W. G. and Didion S. P. (1995) Activation of protein kinase C does not participate in disruption of the blood–brain barrier to albumin during acute hypertension. *Brain Res.* **696**, 106–112.
30. Mayhan W. G. and Didion S. P. (1996) Glutamate-induced disruption of the blood–brain barrier in rats. *Stroke* **27**, 965–970.
31. Moore P. K., Babbege R. C., Wallace P., Gaffen Z. A. and Hart S. L. (1993) 7-Nitro indazole, an inhibitior of nitric oxide synthase, exhibits anti-nociceptive activity in the mouse without increasing the blood pressure. *Br. J. Pharmac.* **108**, 296–297.
32. Morita-Tsuzuki Y., Bouskela E. and Hardebo J. E. (1993) Effects of nitric oxide synthesis blockade and angiotensin II on blood flow and spontaneous vasomotion in the rat cerebral microcirculation. *Acta physiol. scand.* **148**, 449–454.
33. Murphy S., Simmons M. L., Agullo L., Garcia A., Feinstein D. L., Galea E., Reis D. J., Minc-Golomb D. and Schwartz J. P. (1993) Synthesis of nitric oxide in CNS glial cells. *Trends Neurosci.* **16**, 323–328.
34. Nicholson C. and Phillips J. M. (1981) Ion diffusion modified by tortuosity and volume fraction in the extracellular microenvironment of the rat cerebellum. *J. Physiol.* **321**, 225–257.
35. Nicholson C. and Syková E. (1998) Extracellular space structure revealed by diffusion analysis. *Trends Neurosci.* **21**, 207–215.
36. Nicholson C. and Tao L. (1993) Hindered diffusion of high molecular weight compounds in brain extracellular microenvironment measured with integrative optical imaging. *Biophys. J.* **65**, 2277–2290.
37. Patlak C. S. and Fenstermacher J. D. (1975) Measurements of dog blood–brain transfer constants by ventriculocisternal perfusion. *Am. J. Physiol.* **229**, 877–884.
38. Rees D. D., Palmer R. M. J. and Moncada S. (1989) Role of endothelium-derived nitric oxide in the regulation of blood pressure. *Proc. natn. Acad. Sci. U.S.A.* **86**, 3375–5578.
39. Rees D. D., Palmer R. M. J., Schultz H. F. and Moncada S. (1990) Characterization of three inhibitors of endothelial nitric oxide synthase *in vitro* and *in vivo*. *Br. J. Pharmac.* **101**, 746–752.
40. Rice M. E. and Nicholson C. (1991) Diffusion characteristics and extracellular volume fraction during normoxia and hypoxia in slices of rat neostriatum. *J. Neurophysiol.* **65**, 264–272.
41. Salter M., Duffy C. and Hazelwood R. (1995) Determination of brain nitric oxide synthase inhibition *in vivo*: *ex vivo* assays of nitric oxide synthase can give incorrect results. *Neuropharmacology* **34**, 327–334.
42. Shepard A. P. and Öberg P. Å. (1990) *Laser-Doppler Blood Flowmetry*. Kluwer, Boston.
43. Silva M. T., Rose S., Hindmarsh J. G., Aislaitner G., Gorrod J. W., Moore P. K., Jenner P. and Marsden C. D. (1995) Increased striatal dopamine efflux *in vivo* following inhibition of cerebral nitric oxide synthase by the novel monosodium salt of 7-nitro indazole. *Br. J. Pharmac.* **114**, 257–258.
44. Sokrab T.-E. O. and Johansson B. B. (1989) Regional cerebral blood flow in acute hypertension induced by adrenaline, noradrenaline and phenylephrine in the consious rat. *Acta physiol. scand.* **137**, 101–105.
45. Southan G. J. and Szabó C. (1996) Selective pharamacological inhibition of distinct nitric oxide synthase isoforms. *Biochem. Pharmac.* **51**, 383–394.
46. Svoboda J. and Syková E. (1991) Extracellular space volume changes in the rat spinal cord produced by nerve stimulation and peripheral injury. *Brain Res.* **560**, 216–224.
47. Syková E. (1992) *Monitoring Neuronal Activity: A Practical Approach.* Oxford University Press, New York.
48. Syková E. (1997) The extracellular space in the CNS: its regulation, volume and geometry in normal and pathological neuronal function. *The Neuroscientist* **3**, 28–41.
49. Tanaka K., Gotoh F., Gomi S., Takashima S., Mihara B., Shihari T., Nogawa S. and Nagata E. (1991) Inhibition of nitric oxide synthesis induces a significant reduction in local cerebral flow in the rat. *Neurosci. Lett.* **127**, 129–132.
50. Traystman R. J., Moore L. E., Helfaer M. A., Davis S., Banasiak K., Williams M. and Hurn P. D. (1995) Nitro-L-arginine analogues. Dose- and time-related nitric oxide synthase inhibition in brain. *Stroke* **26**, 864–869.
51. Ueki A., Rosén L., Andbjer B., Agnati L. F., Hallström Å., Goiny M., Tanganelli S., Ungerstedt U. and Fuxe K. (1993) Evidence for a preventive action of the vigilance-promoting drug modafinil against striatal ischemic injury induced by endothelin-1 in the rat. *Expl Brain Res.* **96**, 89–99.
52. Vorisek I. and Sykova E. (1997) Ischemia-induced changes in the extracellular space diffusion parameters, K^+, and pH in the developing rat cortex and corpus callosum. *J. cerebr. Blood Flow Metab.* **17**, 191–203.
53. Wadhwani K. C. and Rapoport S. I. (1990) Blood flow in the central and peripheral nervous system. In *Laser-Doppler Blood Flowmetry* (eds Shepard A. P. and Öberg P. Å.), pp. 265–288. Kluwer, Boston.
54. Yang S.-N., Narvárez J. A., Bjelke B., Agnati L. F. and Fuxe K. (1993) Microinjections of subpicomolar amounts of NPY(13–36) into the nucleus of the tractus solitarius of the rat counteract the vasodepressor responses of NPY(13–36) and of an NPY Y_1 receptor agonist. *Brain Res.* **62**, 126–132.
55. Zoli M., Zini I., Agnati L. F., Guidolin D., Ferraguti F. and Fuxe F. (1990) Aspects of neural placticity in the central nervous system. I. Computer-assisted image analysis methods. *Neurochem. Int.* **16**, 383–418.

(*Accepted* 28 *September* 1998)